Izvestiya, Atmospheric and Oceanic Physics, Vol. 41, No. 6, 2005, pp. 741–749. Translated from Izvestiya AN. Fizika Atmosfery i Okeana, Vol. 41, No. 6, 2005, pp. 814–823.

Mesospheric Temperature Inversions from CRISTA-1 Data

V. S. Kostsov and Yu. M. Timofeev

Institute of Physics, St. Petersburg State University,
ul. Ul'yanovskaya 1, Petrodvorets, St. Petersburg, 198504 Russia
e-mail: vlad@troll.phys.spbu.ru; tim@troll.phys.spbu.ru

Received December 1, 2004; in final form, March 24, 2005

Abstract—Characteristics of mesospheric temperature inversions (MTIs) remotely sensed in the CRISTA-1 experiment (November 1994) are analyzed. The original dataset consisted of about 900 vertical temperature profiles in the range of altitudes from 40 to 120 km. MTIs were observed in 84% of cases. One and two inversions were mainly observed (in 40% and 37% of cases, respectively). Profiles with three inversions occurred in about 7% of cases. Profiles with four inversions accounted for less than 1% of cases. Multiple inversions were observed mainly in the equatorial region and in the Northern Hemisphere. The mean amplitude of inversions for the whole dataset is 24.3 K, with the most probable value of 7 K. When only MTIs with a maximum amplitude are taken into account in the case of multiple inversions, the mean amplitude is 30.6 K and the maximum of the frequency distribution of amplitudes lies in the range from 20 to 30 K. Inversions with an amplitude of 80–90 K were also detected. The maximum amplitude was 104 K. Zonal mean amplitudes in 5° latitudinal zones have maxima in the equatorial region and in the midlatitudes (at 30°–40° S and around 50° N). The maximum of the frequency distribution of the vertical extent of inversions is 5 to 7.5 km. No inversions with a vertical extent greater than 15 km were observed. Zonal mean vertical extents of inversions have minima south of 45° S. Zonal mean altitudes of inversions (altitudes of a temperature maximum) decrease sharply from 87.5 km in the southern latitudes to 80–82.5 km at the equator. In the northern latitudes, the inversion altitudes increase only slightly.

1. INTRODUCTION

Mesospheric temperature inversions (MTIs) were first detected in rocket-based observations [1]. Later, these features of the temperature regime of the mesosphere were studied using rocket, ground-based-lidar, and satellite measurements. The main features of MTIs were analyzed in a number of papers, including reviews [2–9]. The following features are noteworthy:

1. MTIs are mainly observed in the low and middle latitudes near 70 and 95 km. It is the lower MTIs that were detected in early rocket measurements [1]. Most measurements apply to the lower MTIs during nighttime at altitudes between 60 and 70 km. This is due to the widespread use of Rayleigh radars (at night) and the method of falling spheres for mesospheric temperature studies. Both these methods have a ceiling of sounding near 80 km.

2. The use of sodium lidars raised the upper limit of measurements to 105 km, thus making it possible to detect a secondary upper inversion layer near 95 km. Nocturnal mesospheric inversions were recorded periodically near 95 km [7], a result which suggested the presence of a double mesopause. In averaging over nighttime and daytime measurements, these inversion layers could hardly be seen.

3. Two nocturnal inversions were often roughly a wavelength of the diurnal tide apart. Each inversion layer is typically 10 km wide.

4. Amplitudes of MTIs relative to the background temperature profile of the mesosphere and lower thermosphere (MLT) usually lie in the range from 10 to 25 K. However, MTIs of much larger amplitude, several tens of degrees, have also been detected.

5. The lower MTIs are a common feature of the MLT temperature structure in winter [10]. MTIs with an amplitude greater than 10 K are observed in over 80% of cases in December and January, but only in 30% of cases during midsummer. The amplitudes greater than 30 K are observed in more than 20% of cases in winter, but they are rare in summer. Monthly mean amplitudes exceed 20 K in winter and are 5–10 K in summer [2, 3]. The altitudes of temperature maxima of the lower inversions are about 75 km in summer and 65 km in winter [2, 4]. The upper MTIs usually have amplitudes from 10 to 35 K and are a common feature of the mesopause region [11]. The ground-based 24-h observations made with a sodium lidar show that MTIs show up very rarely in the diurnal mean temperature profiles, but they are seen clearly in individual temperature profiles with time averaging of the measurements of several minutes. These features indicate that the upper MTIs are related to the tides [7, 8].

Many dynamic, chemical, and radiative processes play an important role in the formation of the thermal structure of the MLT region. Despite a great deal of research, the nature of MTIs is not yet completely clear.

The development of possible mechanisms for MTI formation is a focus of many studies (see, e.g., the reviews mentioned above and [9, 12–16]). Different mechanisms have been proposed for MTIs: dynamic (tides, interaction between tides and gravity or planetary waves, heating through the turbulence generated during the breaking of gravity waves, etc.) and chemical. However, it is unclear, for example, whether the formation of the lower and upper mesospheric inversions is caused by the same mechanisms. Many of the global upper-atmosphere models describing the influence of tides on MTI formation give amplitudes much smaller than the measured ones. Consideration for the interaction between atmospheric tides and gravity and planetary waves makes it possible to obtain inversion amplitudes much better consistent with experimental data. A chemical mechanism of MTI generation [17, 18] may be responsible for the upper MTIs because the chemical-heating rates at altitudes near 90 km can reach 5–10 K per day.

The difficulties in understanding the nature of MTIs are related largely to the fact that MTI observations are fragmentary, a condition which is caused by the use of different experimental methods to study the MLT temperature regime. These methods differ in altitude ranges of measurements, errors, measurement times during the day, and spatial (vertical and horizontal) and temporal resolution. The diurnal averaging of the MLT temperatures substantially complicates analysis of the tidal mechanisms of MTI generation.

In this regard, measurements of vertical temperature profiles made over a wide range of altitudes and with high temporal resolution, which is achieved by using satellite remote sensing methods, are important for analysis of MTIs. Satellite measurements provide the opportunity to study the spatial distribution of MTIs on a global scale. Because of the short scanning time of the planet's limb (seconds and minutes) during a recording of the outgoing radiation, the data obtained can be regarded as instantaneous. The subsequent averaging of satellite data makes it possible to study MTI climatology.

Satellite studies of the mesospheric temperature were started in the experiments aboard the SME in 1982–1986 [19, 20]. Analysis of the measurements made by the ISAMS satellite instrument [21] has shown that lower MTIs have a different lifetime and different spatial extents. Most of them are sporadic, but some may last several days and cover large areas in the horizontal (millions of square kilometers). The ISAMS and HALOE measurements [3, 21] show considerable latitudinal and longitudinal variations in the amplitude of the lower MTIs. Analysis of the ISAMS data for the Northern Hemisphere in December 1991 allowed the authors of [21] to draw the following conclusions:

1. MTIs are present somewhere in the hemisphere almost every day (mainly in a midlatitude belt).

2. The amplitude of the inversions may reach more than 20 K.

3. The horizontal extent of the MIT regions varies from 10^5 to 10^6 km^2.

Study [3] confirmed the existence of the midlatitude belt of strong inversions (with an amplitude as large as 40 K locally and about 10 K for the lower MTIs at altitudes from 70 to 75 km during winter for the monthly means) and the presence of a low-latitude belt of strong inversions of the same amplitude at 80–85 km a few weeks after the equinoxes. Annual variations in the inversion layers were also detected in the middle latitudes, and semiannual variations were found near the equator.

The inversion layers formed by various wave processes were discussed in several studies devoted to analysis of the data from the CRISTA satellite experiments [22–26].

A disadvantage of satellite measurements is their relatively low spatial resolution. Whereas the vertical resolution of these measurements can still be regarded as acceptable (2–4 km), the horizontal smoothing (due to atmospheric self-radiation or absorption on tangent paths and to the movement of the satellite during one scan) is 200–400 km or more depending on the vertical resolution of the instrument. The horizontal resolution of the retrieved profiles in the CRISTA experiments, for example, is estimated at 200 km × 650 km [22]. The smoothing effect of satellite measurements manifests itself, in particular, in an underestimation of MTI amplitudes. In [21], it is pointed out that the amplitudes of inversions measured by satellites may be two to three times smaller than the values observed by ground-based lidars. Nonetheless, new satellite measurements of the vertical temperature profiles in the MLT region provide the opportunity to derive important information about spatial and temporal variations of MTIs and thus to facilitate the development of adequate models for MTIs.

In this paper, we analyze vertical temperature profiles of the MLT region retrieved from the outgoing limb radiation measurements in the 15 μm band of CO_2 made by the CRISTA instrument in November 1994 [27, 28].

2. TEMPERATURE DATA FROM THE CRISTA-1 EXPERIMENT

In [27, 28], the initial data are described in detail, the original technique of interpretation of the CRISTA-1 measurements of the nonequilibrium outgoing radiation in the CO_2 15-μm band is presented, and examples of analysis of the MLT thermal regime are given. The data on MTIs are presented in [28] from analysis of a limited volume of the results of interpretation of the CRISTA measurements, such as altitudes, thicknesses, and amplitudes. It is noted that there were numerous MTIs reaching 50 K. In the present paper, the occur-

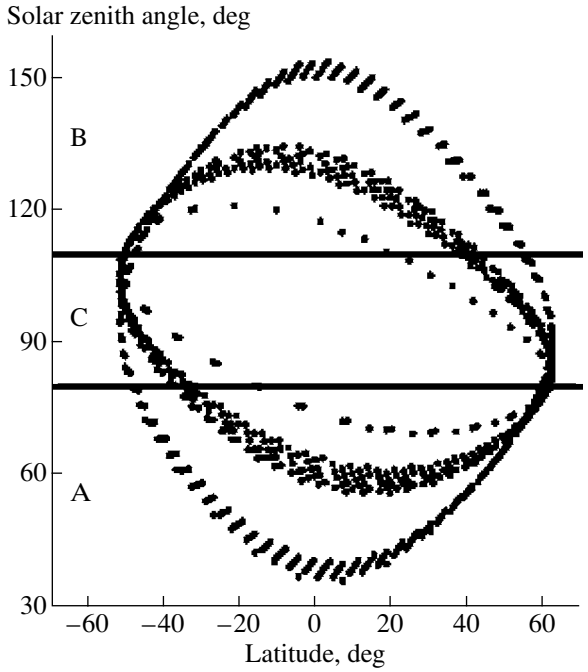

Fig. 1. Distribution of measurement points in latitude and solar zenith angle. Measurements during day (A), during night (B), and at twilight (C) are marked by contours.

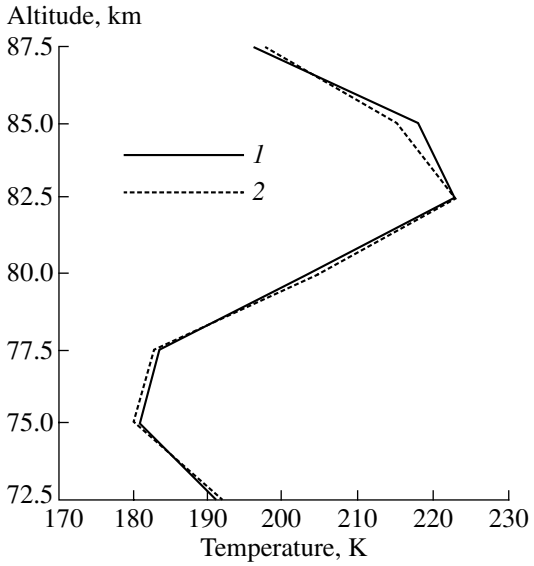

Fig. 2. Retrieval of an MTI in a numerical experiment: (*1*) the retrieved profile and (*2*) the model profile.

rence and characteristics of MTIs are studied for the entire dataset of the CRISTA-1 measurements.

The data analyzed in this paper were obtained on November 4–5 and 8–12, 1994. The total number of temperature profiles was 881. Most of the measurements (approximately 650 profiles) were made on November 5 and 9. The latitudinal range of measurements was from 51.8° S to 62.3° N. The latitude and the solar zenith angle for the entire dataset are displayed in Fig. 1. It can be seen that measurements in the middle latitudes were taken mainly at sunset and sunrise and in the equatorial region during day and night.

Figure 2 shows the results of MTI retrieval in a numerical experiment. The model profile was characterized by an inversion with a vertical extent of 7.5 km and an amplitude of 42.8 K. The retrieved amplitude was 42.0 K. As this example shows, the smoothing effect of the operator of the solution to the inverse problem is negligible. An evident smoothing of temperature perturbations was observed in the numerical experiments at altitudes above 100 km.

In this paper, MTI identification in the temperature data was performed by the following criteria: the altitude of the beginning of an inversion is within the mesosphere and the amplitude of the inversion is greater than 5 K.

The stratopause and mesopause altitudes were determined from the absolute maximum and minimum of temperature in the corresponding height ranges. The zonal mean altitudes of the stratopause and mesopause are shown in Fig. 3. The stratopause altitude is about 48 km between 50° S and 20° N. In the midlatitudes of the Northern Hemisphere, the stratopause altitude increases with latitude, reaching 52 km at 60° N. The mesopause altitude increases from the southern to northern latitudes (from 88 to 102 km), a phenomenon which corresponds to a low cold mesopause in summer and a high warm mesopause in winter. During analysis of inversions, it was assumed that the base of the mesosphere was 10 km above the stratopause in order to eliminate possible events with a double stratopause. Thus, the actual range of altitudes was from 58–62 to 90–100 km.

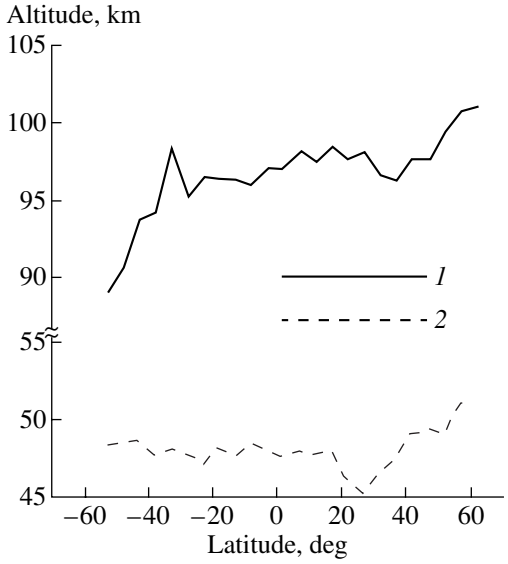

Fig. 3. Altitude of (*1*) mesopause and (*2*) stratopause from CRISTA data.

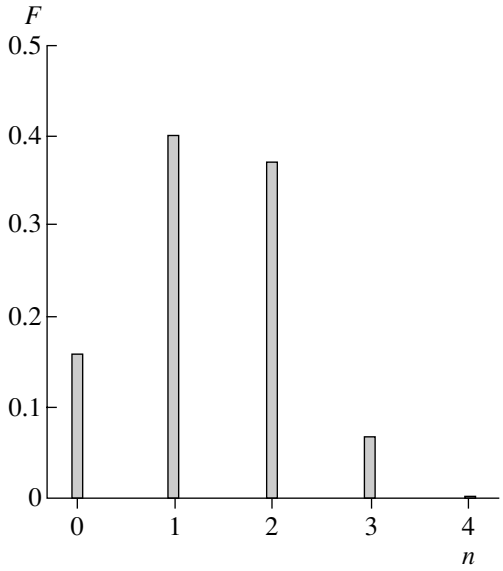

Fig. 4. Relative frequency of occurrence (F) of a different number of inversions (n) in the temperature profile.

3. ANALYSIS OF MTI CHARACTERISTICS

In this paper, the following main characteristics of MTIs are presented and discussed: the amplitude of an inversion (the temperature difference between the top and the base of the inversion), the vertical extent (the difference between the altitudes of the temperature maximum and minimum), the altitudes of the temperature minimum and maximum, the temperature minimum, and the temperature maximum.

The set of the data analyzed contains a large number of temperature profiles with multiple inversions. Figure 4 shows the relative frequency of the occurrence of a different number of inversions in the temperature profile. No inversions were observed in 16% of the total number of profiles. There were mainly one or two inversions in 40% and 37% of cases, respectively. Profiles containing three inversions were observed in about 7% of cases. Profiles with four inversions made up less than 1%.

Because the dataset included profiles with different numbers of inversions, analysis was made for the following three groups: (A) all inversions, (B) only inversions with a maximum amplitude in the case of several inversions in one profile, (C) and only profiles with single inversions.

The relative frequency of inversions of different amplitudes for the three groups indicated above is shown in Fig. 5. In group A, the most frequently observed inversions are the ones with an amplitude of 7 K. The relative frequency decreases with amplitude. There are inversions with amplitudes as large as 80–90 K. One profile contains an inversion with an amplitude of 104 K. The mean amplitude is 24.3 K.

The distribution of amplitudes in group B is quite different. Inversions with amplitudes from 20 to 30 K

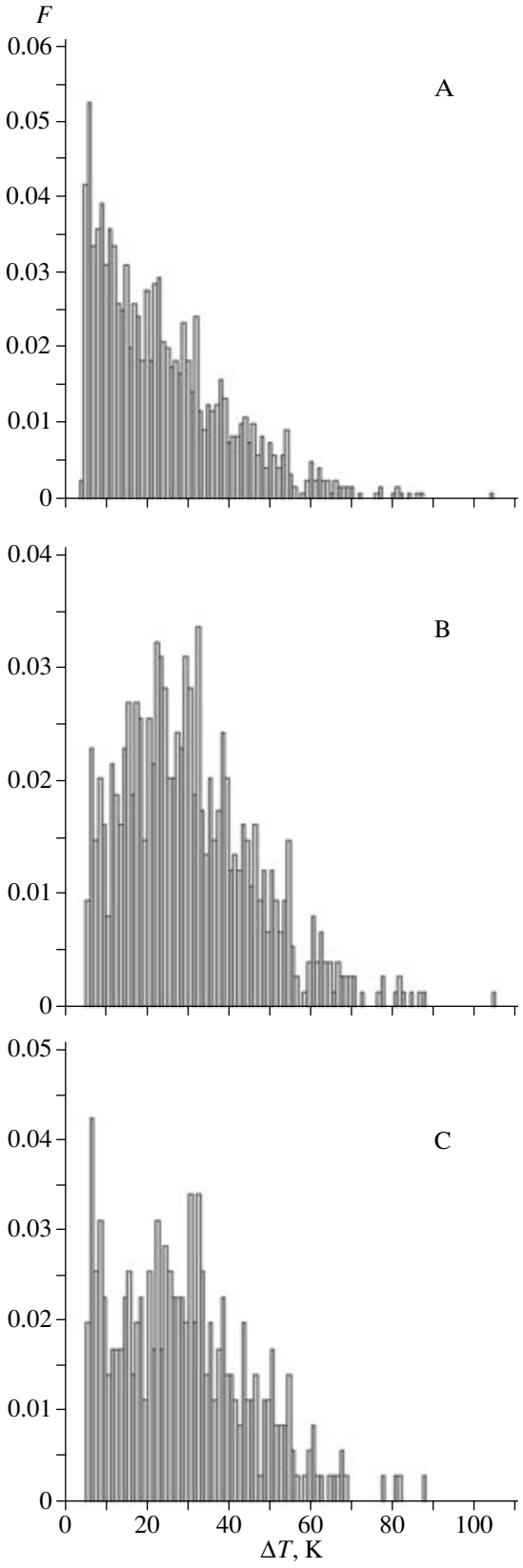

Fig. 5. Relative frequency of occurrence (F) of inversions of different amplitude (ΔT) for groups of data A, B, and C.

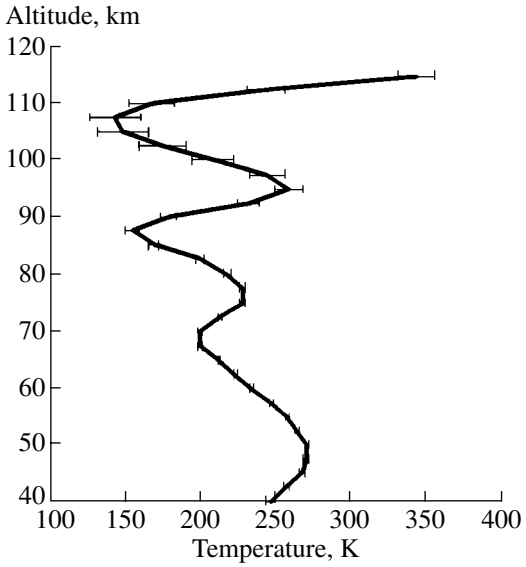

Fig. 6. Temperature profile with the maximum measured amplitude of inversion. Scan 10 172; 4.7° S, 52° W; solar zenith angle 60°.

are observed most frequently. The mean amplitude for such a choice of data is 30.6 K.

The distribution of the relative frequency of inversions of different amplitudes for group B, shown in Fig. 5 at the bottom, has two distinct maxima. A narrow maximum corresponds to amplitudes in the range from 6 to 8 K. A broad maximum spans the range from 20 to 32 K. For the third group of data, the mean amplitude of inversions is 28.9 K.

Figure 6 gives an example of the retrieved temperature profile with a maximum amplitude of inversion of 104 K (scan 10 172; November 9, 1994; measurement-point coordinates 4.7° S, 52° W; zenith angle 60°). The profile shown in Fig. 6 contains two mesospheric inversions. The lower inversion has an amplitude of 30 K.

Figure 7 shows the relative frequency of inversions of a different vertical extent for the three groups of data. In all groups, inversions with a vertical extent from 5 to 7.5 km are most probable. Note that the altitude-grid step in the retrieval of temperature profiles was 2.5 km. No inversions with a vertical extent larger than 15 km were observed.

Since the vertical extent of inversions is variable, the altitudes of inversions were estimated from the altitude of the temperature maximum. Figure 8 shows the frequency distribution of inversion altitudes for the analyzed groups of data. In group A, a broad maximum of the occurrence frequency corresponds to the altitude range from 75 to 95 km. Below 75 km, the relative frequency of the occurrence of inversions is low. When only inversions of maximum amplitude are considered in the case of multiple inversions (group B), the frequency distribution is close to a symmetric distribution and has a maximum at altitudes between 82.5 and 87.5 km. The

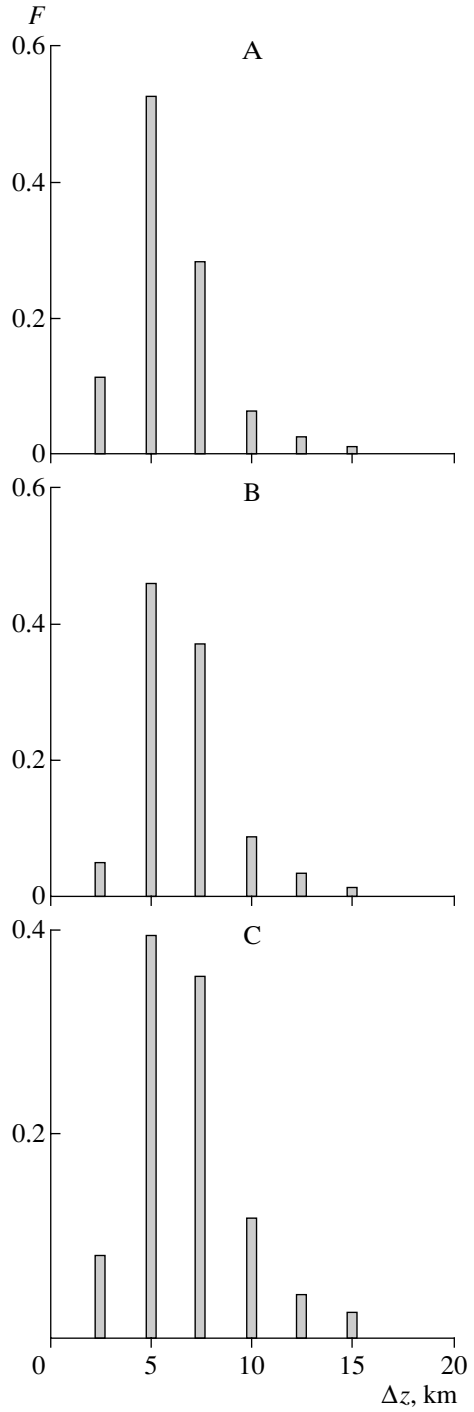

Fig. 7. Relative frequency of occurrence (F) of inversions of a different vertical extent (Δz) for groups A, B, and C.

ensemble of single inversions (group C) has a narrower frequency distribution. Practically no single inversions were observed below 75 km and above 95 km.

Calculations of zonal mean characteristics of MTIs were carried out for 5° latitudinal zones. The table presents the number of inversions by latitudinal zones in the analyzed groups of data. The number of measured

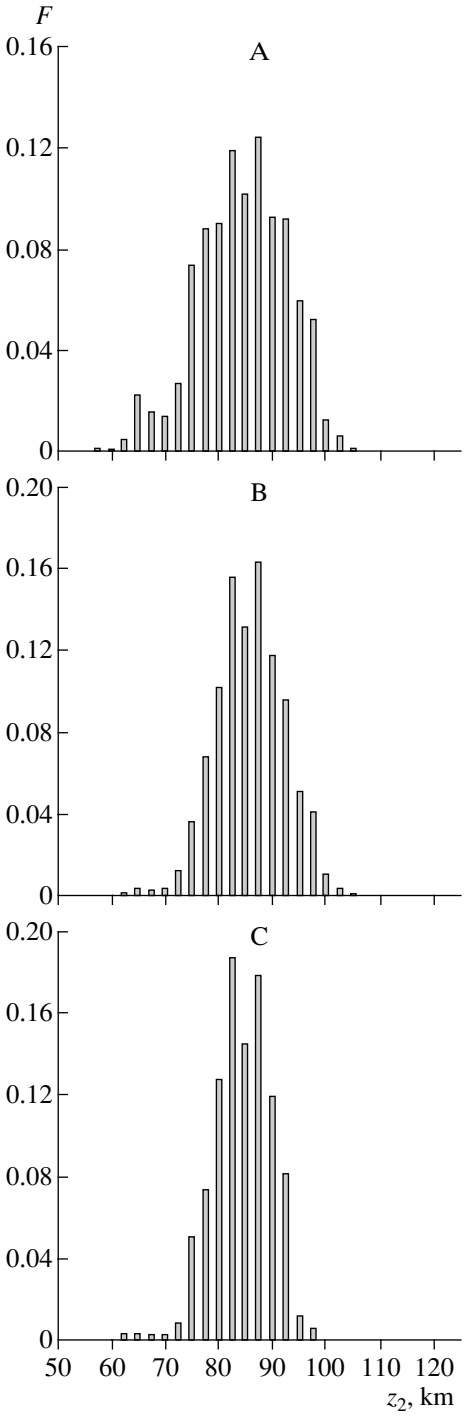

Fig. 8. Relative frequency of occurrence (F) of inversions with a different altitude of the temperature maximum (z_2) for groups A, B, and C.

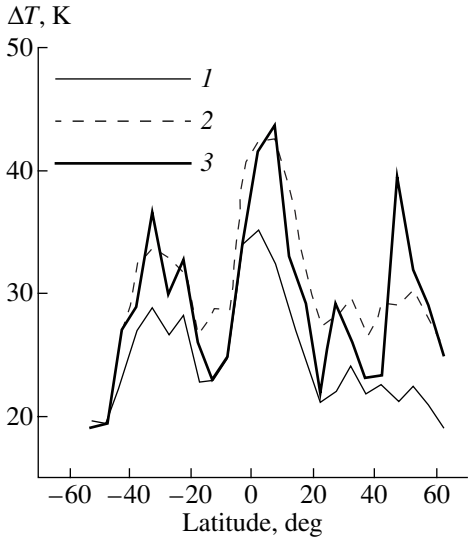

Fig. 9. Zonal mean amplitudes of inversions (ΔT) for groups A (*1*), B (*2*), and C (*3*).

temperature profiles is given there for comparison. (The amount of data in group A is larger than the number of measured profiles in most zones owing to the presence of multiple inversions.) As can be seen from the table, single inversions are observed mainly in the latitudinal zone 45°–55° S. For the most part, multiple inversions are observed in the Northern Hemisphere. In all groups of data, the number of inversions in the latitudinal zones is sufficient to calculate the zonal mean characteristics of MTIs.

The zonal mean amplitudes of inversions are shown in Fig. 9. For the entire dataset (group A) and for the group containing only maximum inversions in the case of multiple MTIs (group B), a typical feature is the presence of two maxima: one in the latitudinal zone 20°–40° S and the other in the equatorial region. In the case of only single inversions (group C), a third maximum appears at 50° N. At the maxima, zonal mean amplitudes reach 35–45 K.

Zonal mean values of the vertical extent of inversions are shown in Fig. 10. The minimum values are observed south of 45° S. The maxima of the vertical extent correspond to the maxima of zonal mean amplitudes.

The zonal mean altitudes of the temperature maximum and minimum are presented in Fig. 11. In the Southern Hemisphere, the altitude of the temperature maximum decreases sharply from 87.5 to 80–82.5 km. In the Northern Hemisphere, the altitude of the inversion maximum increases only slightly. The latitudinal variation in altitude of temperature maximum is almost identical for all the groups analyzed. In general, the latitudinal dependence of the altitude of the temperature minimum is analogous to that of the altitude of maximum. However, in group C (single inversions), the altitudes of the temperature minimum in the equatorial regions are smaller than those in other groups of data.

Finally, consider the zonal mean numbers of inversions n in the temperature profile (Fig. 12). It can be seen that many of the profiles without inversions ($n < 1$) are located south of 40° S. The number of inversions increases monotonically from the Southern Hemi-

sphere toward the Northern Hemisphere. The maximum value of n is 1.9, a value which suggests the presence of primarily multiple inversions at 60° N.

4. DISCUSSION AND CONCLUSIONS

The characteristics of MTIs will be compared with lidar observations at Observatoire de Haute-Provence (OHP; 44° N, 5° E) and Centre d'Essais des Landes (CEL; 44° N, 1° W) and with results obtained in the ISAMS and HALOE satellite experiments [3]. The lidar and satellite observations have a long duration and give information about the seasonal dependence of MTI parameters. The shortness of the CRISTA-1 experiment does not allow the study of MTI temporal characteristics. The time of measurements (November 1994) may be treated as the beginning of the winter period in the Northern Hemisphere and the beginning of the summer period in the Southern Hemisphere. During comparison of the results, one should keep in mind that the ceiling of lidar and satellite measurements was found to be 85–90 km [3] and, at this altitude, the errors in the lidar temperature measurements were estimated at 2%, while those in the ISAMS and HALOE measurements were estimated at about 15 K. The temperature profiles were smoothed strongly in the satellite measurements. In the CRISTA-1 experiment, the temperature was determined up to 120 km. Thus, MTIs were observed up to altitudes of the mesopause (100 km in midlatitudes). The total error at 90 km was 5.5 K. (The random component was 3.7 K, and the systematic one was 4.0 K.) As was shown above, the smoothing effect during processing of the CRISTA-1 measurements is negligible. These differences in measurement periods, altitude ranges, and errors must be taken into account when comparing the results.

Two main conclusions drawn from analysis of lidar observations and satellite measurements (ISAMS and HALOE) in [3] are (1) the occurrence of a midlatitude belt of strong inversions with local amplitudes of 40 K and monthly mean amplitudes of 10 K between the altitudes of 70 and 75 km during winter and (2) the occurrence of a low-latitude belt of strong inversions with the same amplitudes occurring between 80 and 85 km a few weeks after the equinoxes. The results of processing the CRISTA-1 measurements agree well with these conclusions: both belts of MTIs have been observed. However, the altitudes of the inversions (altitudes of the temperature minimum) in our case are somewhat different: about 77.5 km in midlatitudes and 75 km in the equatorial zone. The CRISTA-1 data are also indicative of strong MTIs occurring in the middle latitudes of the Southern Hemisphere at about 82.5 km.

The monthly mean amplitude of MTIs in November from lidar measurements (at 44° N) is about 20 K. The mean amplitudes obtained in our study for three groups of data (A, B, and C) are about 20, 29, and 40 K, respectively. It should be stressed that, owing to a substantial smoothing of the profiles, the inversion amplitudes from the ISAMS and HALOE data are much smaller than the CRISTA-1 amplitudes.

Number of inversions in latitudinal zones in analyzed groups of data (see text)

Latitudinal zone	Total number of temperature profiles	Number of inversions in groups of data		
		A	B	C
55° S–50° S	58	15	14	13
50° S–45° S	61	26	26	26
45° S–40° S	42	38	30	22
40° S–35° S	35	35	25	15
35° S–30° S	34	41	31	21
30° S–25° S	29	37	24	13
25° S–20° S	31	37	28	20
20° S–15° S	29	42	29	18
15° S–10° S	30	45	28	13
10° S–5° S	27	45	27	9
5° S–0°	31	46	30	15
0°–5° N	27	41	27	13
5° N–10° N	34	56	34	16
10° N–15° N	31	54	30	11
15° N–20° N	32	52	31	14
20° N–25° N	29	47	26	9
25° N–30° N	30	49	26	8
30° N–35° N	32	48	31	18
35° N–40° N	33	51	31	13
40° N–45° N	35	55	32	10
45° N–50° N	35	56	32	10
50° N–55° N	40	68	38	12
55° N–60° N	54	102	52	13
60° N–65° N	62	110	60	21

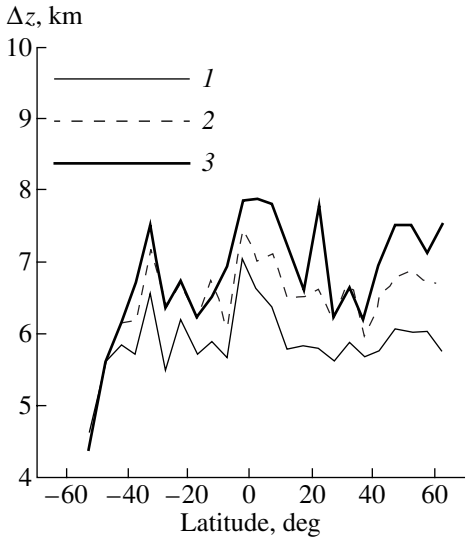

Fig. 10. Zonal mean vertical extent of inversions (Δz) for groups A (*1*), B (*2*), and C (*3*).

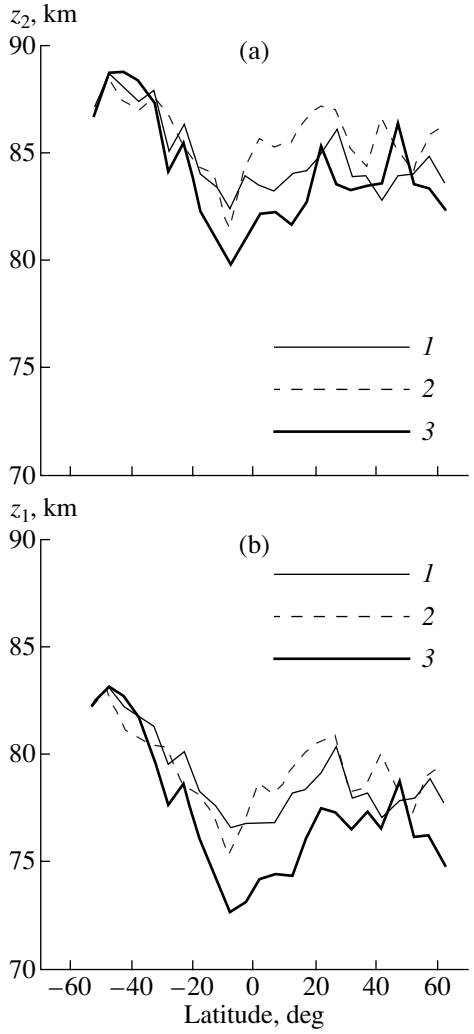

Fig. 11. Zonal mean altitude of (a) the temperature maximum and (b) the temperature minimum for groups A (*1*), B (*2*), and C (*3*).

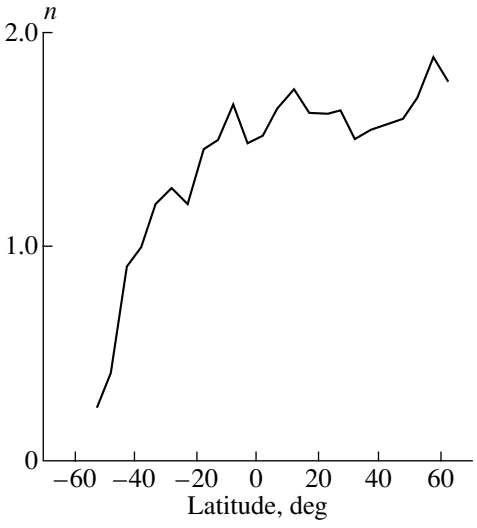

Fig. 12. Zonal mean number of observed inversions (n) in the temperature profile.

From lidar measurements, the mean temperature lapse rate in a mesospheric inversion is independent of the season and equals 3–5 K/km. The corresponding values obtained for different groups of data are (A) 4.1 K, (B) 4.7 K, and (C) 4.3 K.

Thus, the results obtained are in good quantitative agreement with lidar observations. Correct intercomparisons with the ISAMS and HALOE measurements are hampered primarily because the temperature profiles in these experiments are smoothed strongly and the altitude ranges being studied are different.

ACKNOWLEDGMENTS

This study was supported by the Russian Foundation for Basic Research, project no. 03-05-64830, and by the Russian Ministry of Education, project no. 01.01.044 of the research program "Universities of Russia."

REFERENCES

1. F. J. Schmidlin, "Temperature Inversions near 75 km," Geophys. Rev. Lett. **3**, 173–176 (1976).
2. A. Hauchecorne, M. L. Chanin, and P. Keckhut, "Climatology and Trends of the Middle Atmospheric Temperature (33–87 km) As Seen by Rayleigh Lidar over the South of France," J. Geophys. Res. D **96**, 15297–15309 (1991).
3. T. Leblanc and A. Hauchecorne, "Recent Observations of Mesospheric Temperature Inversions," J. Geophys. Res. D **102**, 19471–19482 (1997).
4. J. A. Whiteway, A. I. Carswell, and W. E. Ward, "Mesospheric Temperature Inversions with Overlaying Nearly Adiabatic Lapse Rate: An Indication of Well-Mixed Turbulent Layer," Geophys. Rev. Lett. **22**, 1201–1204 (1995).
5. J. R. Yu and C. Y. She, "Climatology of a Midlatitude Mesopause Region Observed by a Lidar at Fort Collins, Colorado," J. Geophys. Res. D **100**, 7441–7452 (1995).
6. J. W. Meriwether, X. Gao, V. B. Wickwar, *et al.*, "Observed Coupling of the Mesospheric Inversion Layer to the Thermal Tidal Structure," Geophys. Rev. Lett. **25**, 1479–1482 (1998).
7. R. J. States and C. S. Gardner, "Thermal Structure of the Mesopause Region (80–105 km) at 40° N Latitude. I. Seasonal Variation," J. Atmos. Sci. **57**, 66–77 (2000).
8. R. J. States and C. S. Gardner, "Thermal Structure of the Mesopause Region (80–105 km) at 40° N Latitude. II. Diurnal Variation," J. Atmos. Sci. **57**, 78–92 (2000).
9. J. W. Meriwether and C. S. Gardner, "A Review of the Mesosphere Inversion Layer Phenomena," J. Geophys. Res. D **105**, 12405–12416 (2000).
10. A. Hauchecorne, M. L. Chanin, and R. Wilson, "Mesospheric Temperature Inversion and Gravity Wave Dynamics," Geophys. Rev. Lett. **14**, 935–939 (1987).
11. C. Y. She, J. R. Yu, and H. Chen, "Observed Thermal Structure of a Midlatitude Mesopause," Geophys. Rev. Lett. **20**, 567–570 (1993).
12. R. L. Walterscheid and G. Schubert, "Nonlinear Evolution of an Upward Propagation Gravity Wave: Overturn-

ing, Convection, Transience and Turbulence," J. Atmos. Sci. **47**, 101–125 (1990).

13. R. J. Sica and M. D. Thorsley, "Measurements of Superadiabatic Lapse Rates in Middle Atmosphere," Geophys. Rev. Lett. **23**, 2797–2800 (1996).
14. L. Thomas, A. K. P. Marsh, D. P. Wareing, *et al.*, "VHF Echoes from the Midlatitude Mesosphere and the Thermal Structure Observed by Lidar," J. Geophys. Res. **101**, 12867–12877 (1996).
15. H.-L. Liu and M. E. Hagan, "Local Heating/Cooling of the Mesosphere Due to Gravity Wave and Tidal Coupling," Geophys. Rev. Lett. **25**, 2941–2944 (1998).
16. H.-L. Liu, M. E. Hagan, and R. G. Roble, "Local Mean State Changes Due to Gravity Wave Breaking and Impacts on Turbulence and Mean State," J. Atmos. Sci. **56**, 2152–2177 (1999).
17. M. G. Mlynczak and S. Solomon, "A Detailed Evaluation of the Heating Efficiency in the Middle Atmosphere," J. Geophys. Res. D **98**, 10517–10541 (1993).
18. J. W. Meriwether and M. G. Mlynczak, "Is Chemical Heating a Major Cause of the Mesosphere Inversion Layer?," J. Geophys. Res. D **100**, 1379–1388 (1995).
19. R. T. Clancy and D. W. Rush, "Climatology and Trends of Mesospheric (58–90 km) Temperature Based upon 1982–1986 SME Limb Scattering Profiles," J. Geophys. Res. D **94**, 3377–3393 (1989).
20. R. T. Clancy, D. W. Rush, and M. T. Callan, "Temperature Minima in the Average Thermal Structure of the Middle Atmosphere (70–80 km) from Analysis of 40- to 92-km SME Global Temperature Profiles," J. Geophys. Res. D **99**, 19001–19020 (1994).
21. T. Leblanc, A. Hauchecorne, M. L. Chanin, *et al.*, "Mesospheric Temperature Inversions As Seen by ISAMS (UARS)," Geophys. Rev. Lett. **22** (12), 1485–1488 (1995).
22. D. Offermann, K.-U. Grossmann, P. Barthol, *et al.*, "Cryogenic Infrared Spectrometer and Telescopes for the Atmosphere (CRISTA) Experiment and Middle Atmosphere Variability," J. Geophys. Res. D **104**, 16311–16325 (1999).
23. M. Riese, R. Spang, P. Preusse, *et al.*, "Cryogenic Infrared Spectrometer and Telescopes for the Atmosphere (CRISTA) Data Processing and Atmospheric Temperature and Trace Gas Retrieval," J. Geophys. Res. D **104**, 16349–16367 (1999).
24. W. E. Ward, J. Oberheide, M. Riese, *et al.*, "Tidal Signature in Temperature Data from CRISTA 1 Mission," J. Geophys. Res. D **104**, 16391–16403 (1999).
25. P. Preusse, B. Schaeler, J. T. Bacmeister, and D. Offermann, "Evidence for Gravity Waves in CRISTA Temperatures," Adv. Space Res. **24**, 1601–1604 (1999).
26. P. Preusse, S. D. Eckermann, J. Oberheide, *et al.*, "Modulation of Gravity Waves by Tides As Seen in CRISTA Temperatures," Adv. Space Res. **27**, 1773–1778 (2001).
27. V. S. Kostsov and Yu. M. Timofeev, "Interpretation of Satellite Measurements of the Outgoing Nonequilibrium IR Radiation in the CO_2 15-μm Band: 1. Description of the Method and Analysis of Its Accuracy," Izv. Akad. Nauk, Fiz. Atmos. Okeana **37**, 789–800 (2001) [Izv., Atmos. Ocean. Phys. **37**, 728–738 (2001)].
28. V. S. Kostsov and Yu. M. Timofeev, "Interpretation of Satellite Measurements of the Outgoing Nonequilibrium IR Radiation in the CO_2 15-μm Band: 2. Processing the CRISTA Experimental Data," Izv. Akad. Nauk, Fiz. Atmos. Okeana **37**, 801–810 (2001) [Izv., Atmos. Ocean. Phys. **37**, 739–747 (2001)].

Translated by N. Tret'yakova